Resonant Two-Photon Detachment through the Lowest Singlet D State in H^-

A. Stintz,[1] Xin Miao Zhao,[2] Charlie E. M. Strauss,[2] W. B. Ingalls,[2] G. A. Kyrala,[2] David J. Funk,[2] and H. C. Bryant[1]
[1]*Department of Physics and Astronomy, University of New Mexico, Albuquerque, New Mexico 87131*
[2]*Los Alamos National Laboratory, Los Alamos, New Mexico 87545*
(Received 6 June 1995)

We report the measurement of the two-photon detachment spectrum of the $^1D^e$ resonance of H^- just below the $n = 2$ threshold. The excess photon detachment resonance fits a Fano profile with energy 10.872(2) eV (relative to H^- ground state), a width of 0.0105(10) eV, and a shape parameter of −8(2). To our knowledge, this describes the first time direct multiphoton excitation of a resonance has been observed in any negative atomic ion.

PACS numbers: 31.50.+w, 32.80.Fb, 32.80.Wr

Excess photon detachment (EPD) from a negative ion occurs when the ejected electron absorbs more photons than are required to liberate it. The two-photon excitation of an autodetaching resonance is thus a resonant EPD process when the single-photon energy exceeds the threshold for detachment. Proulx, Pont, and Shakeshaft have calculated the rates for electron production by resonant two-photon absorption in the continuum just below the threshold for breakup of the H^- ion into a neutral H in $n = 2$ and a free electron [1,2]. The suggestion that these doubly excited resonances [3] could be accessed by a two-photon process in the EPD regime was first given by Crance [4,5], and has been discussed by Stapelfeldt and Haugen [6,7]. In this paper we report the observation of the $^1D^e$ state in H^-, lying about 72 meV below the $n = 2$ threshold.

Although the lowest resonances in H^- (^1S, ^3P, and ^1D) have been studied in electron transmission spectroscopy [8], previous work in experimental photoexcitation of the resonance region of H^- has been restricted to the study of $^1P^o$ states, which are the only states accessible by a single photon dipole transition from $^1S^e$ ground state. However, as analyzed by Callaway and Rau [9] and demonstrated by Bryant *et al.* [10] and Gram *et al.* [11], in studying the single-photon absorption spectrum in a strong electric field, the presence of ^1S and ^1D resonances with even parity can be inferred through their Stark mixing with neighboring, odd parity, ^1P resonances. For fields above 700 kV/cm, a split structure can clearly be discerned in the photodetachment spectrum that is attributed to the Stark mixed $^1D^e$, lying about 110 meV below the broadened $^1P^o$ shape resonance [10]. This Stark-induced structure in the $^1P^o$ continuum arises from the same $^1D^e$ resonance whose direct observation in the two-photon spectrum is reported in this paper.

Briefly, the experimental setup is as follows (Fig. 1). The 4X H^- Penning ion source developed for the Ground Test Accelerator (GTA) [12] at Los Alamos National Laboratory provides a 46 mA H^- beam accelerated to 35 kV and operating at 5 Hz. The H^- flux is reduced to approximately 4 μA by aperturing the beam. The H^- beam is relayed via an Einzel lens through a cylindrical samarium-cobalt permanent magnet with a peak magnetic field of 2700 G that forms the entrance to a magnetic bottle time-of-flight (TOF) electron spectrometer of the Kruit-Read [13] design as modified by Kyrala [14].

A laser beam intersects the H^- flux about 3 mm beyond the exit from the permanent magnet near the peak of the magnetic field. The laser is polarized along the ion beam and operates at wavelengths near 228 nm. The UV light is generated by mixing in a β-BBO nonlinear crystal the third harmonic of an Nd:YAG with the output of a dye laser operating near 640 nm (DCM dye) pumped by the second harmonic from the same YAG. The resulting 7 ns pulse has an energy of 3 mJ. The laser is focused onto the ion beam using a combination of spherical and cylindrical lenses to achieve a thin 10 μm wide spot along the beam direction with a height of 100 μm (perpendicular to the ion and laser beam paths), providing intensities near 3×10^{10} W/cm^2. Laser frequency calibration was carried out using a 1 m monochromator with a 2400 lines/mm grating operating in first order. The monochromator was calibrated using a mercury pen lamp.

The photodetached electrons are deflected adiabatically from the H^- and H atoms along the field lines connecting the permanent magnet to the solenoidal field within the

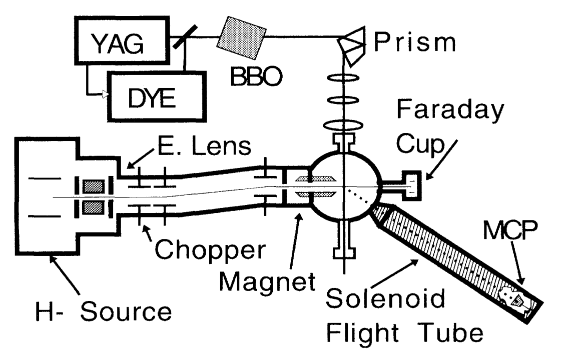

FIG. 1. A schematic of the experimental arrangement. The magnetic bottle is an adaptation of a Kruit-Read design modified by Kyrala [13,14].

 0031-9007/95/75(16)/2924(4)$06.00

flight tube. The electrons travel approximately 1 m and are detected with a two-stage microchannel plate (MCP). The 7 ns laser pulse width, the adiabatic bend in the magnetic field, and the electron detector response time limit the temporal resolution of the TOF spectrometer to several ns. The transient output is integrated for 2000 laser shots with a digital scope. To record a TOF spectrum for the two-photon signal the scope is made to act as a discriminator by setting the baseline voltage level 3 mV outside the digitized range of the scope.

Under typical experimental conditions, each laser shot produces several thousand photodetached electrons from nonresonant one-photon detachment; even at the peak of the two-photon $^1D^e$ resonance less than 30 two-photon detached electrons are observed per shot. In order to detect the very low count rate due to two-photon detachments, considerable efforts were necessary to reduce the background count rate below 1 MHz. With no beam, the TOF region is pumped down to less than 10^{-8} Torr and operates near 2×10^{-8} Torr during experiments to minimize spurious counts from ions and electrons scattered by impact with the background gas. The TOF solenoid, dissipating 200 W, is cooled to reduce the outgassing rate in the flight tube. Additionally, the 400 μs H^- pulse from the ion source is gated down to 100 ns with a pulsed transverse electric field, reducing the background count rate arising from collisions of the ion beam with residual gas. The beam is also cleared of unwanted neutral atoms and electrons by a second transverse electric field that bends the H^- through the permanent magnet. We reduce stray UV light, to which the detector is sensitive, by placing baffles along the magnetic flight tube walls and by coating the tube with graphite. This is essential both for reducing the background photoelectron rate and for preventing distortion of the signal due to charge depletion in the MCP. No energy-selecting repeller grids are used in the TOF tube as we found that they increased our background count rate, perhaps from secondary electron emission.

In the rest frame of the ion beam, the photodetached electron acquires a kinetic energy $T_e = Nh\nu - E_b$, where N is the number of photons absorbed, h is Planck's constant, ν is the frequency of the laser, and E_b is the binding energy of the detached electron. In the Kruit-Read spectrometer the orbit of the spiraling electrons increases as the magnetic field lines diverge from the high field region to the low field of the solenoid. For a large expansion ratio, this effectively deflects the total kinetic energy of the electrons into a kinetic energy along the flight tube axis given by

$$T = T_0 + T_e + 2\sqrt{T_0 T_e}\cos(\theta), \quad \text{with } T_0 = \frac{m v_0^2}{2}, \tag{1}$$

where m is the mass of the electron, v_0 is the ion beam velocity, and θ is the angle between the ion beam velocity and the electron velocity vectors in the ion beam rest frame. This maps the electron velocity angular distribution into an arrival time at the detector. After a flight distance d, the rate of electrons arriving at time t is given by

$$I = \frac{\pi}{\sqrt{T_e T_0}} \frac{m d^2}{t^3} \frac{\sigma}{4\pi} \left[1 + \sum_{k=1}^{N} \beta_{2k} P_{2k}(\cos(\theta)) \right], \tag{2}$$

where σ is the detachment yield. The summation in Eq. (2) is a general expansion in Legendre polynomials P for the angular distribution of electrons with the laser linearly polarized along the ion beam velocity vector [15]. Since we excite to resonances with well-defined angular momentum states, this formula reduces to the spherical harmonic probability distribution corresponding to the angular momentum state of the ejected electron (see below). For one- and two-photon absorption, we need to consider only the first two terms of the series ($k < 3$).

Shown in Fig. 2(a) is an averaged (2000 shots) TOF distribution. The early time feature is due to residual stray light striking the MCP and marks $t = 3$ ns on the trace. The larger extended feature is from the one-photon detachment of the H^- ion at 228 nm. This characteristic temporal profile arises in the laboratory frame due to the addition of the velocity vector distribution of the electron ejection with the center of mass velocity of the ion beam [cf. Eq. (2) containing only the $k = 1$

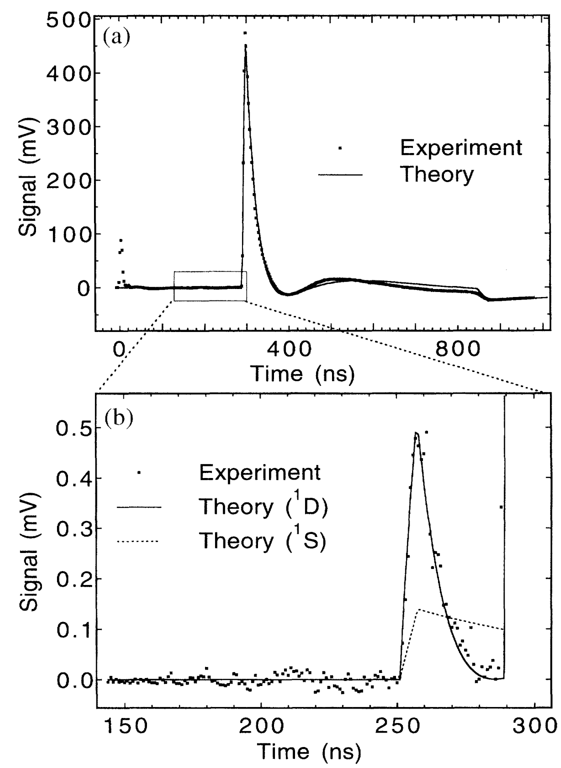

FIG. 2. (a) A typical time-of-flight electron spectrum for the one-photon detachment process. The temporal distribution reflects the angular distribution for a given center of mass electron energy. (b) An enlarged view (~1000×) of the rectangular area of (a) shows the portion of the two-photon signal that we observe in these experiments.

term (p wave)]. In a one-photon dipole detachment process starting and ending in a spherically symmetric atomic state [i.e., $H^- \, {}^1S^e \rightarrow H^0(1s)^2S$], the selection rule requires that the angular momentum state of the ejected electron be described by the Y_{10} spherical harmonic quantized along the polarization axis. This corresponds to $\beta_2 = 2$ in Eq. (2). The data for the one-photon absorption are fit well using this asymmetry parameter. (This fit incorporates the instrument response function.)

Shown in Fig. 2(b) is a blowup of the temporal region preceding the single-photon distribution where we expect to see the onset of the two-photon detached electrons. This signal is smaller by a factor of 10^3 than the one-photon result, and in fact corresponds to only a few electrons per laser pulse. The temporal profile observed is energetically [see Eq. (1)] consistent with two-photon excitation of H^- followed by detachment leaving the neutral atom with the final state of ${}^2S$. Two-photon detached electrons have a greater excess energy than the one-photon detached electrons in the ion center of mass frame, but only those faster in the lab frame are unobscured. For a d-wave angular distribution, approximately 30% of the electrons will have sufficient forward kinetic energy to be distinguished from the one-photon electrons.

We can determine the symmetry of the ion state from the shape of the TOF wave form. The dipole selection rules restrict the angular distribution of the detached electrons to a Y_{20} spherical harmonic if the ion is excited to a D state, or to a Y_{00} if the ion is excited to an S state. The TOF transient wave form corresponding to $|Y_{20}|^2$ is a reasonable fit to the observed TOF two-photon spectrum as shown in Fig. 1(b). In contrast, the TOF transient wave form corresponding to $|Y_{00}|^2$, also shown in the figure, is a poor fit. Thus we conclude that the excited H^- state is the ${}^1D^e$ state and not the ${}^1S^e$ state. $|Y_{20}|^2$ corresponds to $\beta_2 = 10/7$ and $\beta_4 = 18/7$ in Eq. (2), while $|Y_{00}|^2$ is isotropic and corresponds to $\beta_2 = \beta_4 = 0$.

Shown in Fig. 3 is an excitation spectrum generated by averaging 1000 TOF transient wave forms at each wavelength and plotting the integrated electron signal vs photon energy. The solid line is a fit to the data using the Beutler-Fano line shape [16]:

$$\sigma(E) = \sigma_a \frac{(q + \epsilon)^2}{(1 + \epsilon^2)} + \sigma_b, \quad \text{with } \epsilon = 2\,\frac{(E - E_0)}{\Gamma}, \tag{3}$$

where E_0 is the resonance pole energy measured from the H^- ground state, Γ is the natural linewidth, q is the line profile index, and σ_a and σ_b are constants. Also shown is the theoretical prediction of the line shape of the two-photon excitation of H^- carried out by Proulx and Shakeshaft for the ${}^1D^e$ state of H^- [1,17]. The measured peak of the resonance is shifted from their calculated peak by approximately 5 meV. This is perhaps not surprising since the calculations do not appear to be optimized for accurate energy determinations (e.g., their calculated electron affinity of H^- deviates approximately 2% from the known electron affinity [18]). However, there is fair agreement between the experimental line shape and the calculated line shape [1]. Table I compares our experimental results to this and other theoretical predictions of the energy level and width of the ${}^1D$ state of H^- [19,20]. The calculations by Ho and Bhatia show good agreement with the experimental peak position [20,21].

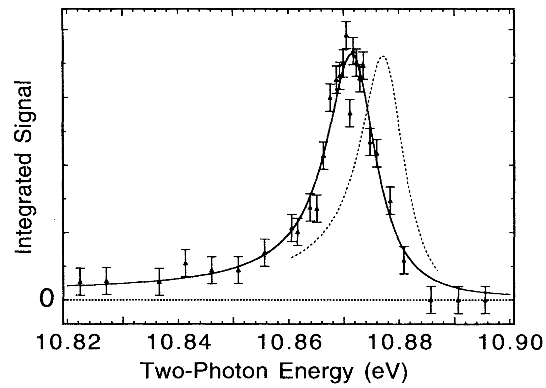

FIG. 3. The yield of electrons in the two-photon detachment continuum in the region of the ${}^1D^e$ resonance as a function of energy. Shown also is the fit to a Fano line profile (solid) and the theoretical prediction of Proulx and Shakeshaft (dashed) [17].

The experimental linewidth is 10% to 20% wider than those predicted. This cannot be accounted for as an artifact of power or transit time broadening, the linewidth of the laser, or the divergence in the ion beam. Our angle-tuned mixing crystal and prism forced us to realign the laser beams to maximize the signal at each wavelength. If this introduced a systematic error, it would most likely appear as an apparent broadening of the profile. However, we believe this effect is also negligible. The width of the line shape calculated by Proulx and Shakeshaft lies within our experimental error [1,17].

In order to maximize the two-photon rate, we examined the coupled rate equations for the one- and two-photon processes. The depletion of the laser beam as it traverses the ion flux is negligible and the depletion of the ion flux due to two-photon excitation is clearly negligible, since we produce at most ten detachments. The suppression of the two-photon process due to the extinction of the

TABLE I. Positions and widths of the ${}^1D^e$ resonance. Reduced Rydberg used to convert from atomic units to eV.

	Energy (eV)	Γ (eV)
This work (experimental)[a]	10.872(2)	0.0105(10)
Ho [21]	10.87291	0.008601
Proulx and Shakeshaft[b] [1]	10.877	0.0096
Bhatia and Ho [20]	10.87304(4)	0.008613(27)
Scholz, Scott, and Burke [19]	10.8739	0.00881

[a] $q = -8(2)$.
[b] Fitted from [17]. $q = -6.9$.

ion beam by the nonresonant single-photon process is not negligible. In the Cs negative ion, Stapelfeldt and Haugen [7] cleverly avoided this concern by exploiting a convenient Fano "window" state where the one-photon detachment rates are inhibited by quantum interference.

It might seem that one could favor the nonlinear electron production process by focusing the laser as tightly as possible. In fact, this is not the case: Focusing to a smaller waist shrinks the Rayleigh range as the square of the waist. Thus, once the Rayleigh range is smaller than the ion beam diameter, gains in ion production due to increased intensity at the focus are offset by the decreased production at the edges of the ion beam. Combining this with the depletion effect, we calculate, for an ion beam diameter of 1 mm and a 3 mJ pulse, that the optimum focus has a waist ~ 10 μm (along the ion trajectory) by ~ 100 μm. Use of this optimal focus, as opposed to focusing as tightly as possible, was critical in reaching a measurable signal level.

The appearance of a resonance profile in the spectrum is very clear evidence that the EPD is essentially a direct one step process rather than the absorption of additional photons after it is detached into the continuum. Refinements of this technique should lead to the observation of other dipole-forbidden transitions including the lower lying ^1S state and the verification of other predicted structures below the $n = 2$ threshold. Two-photon access to this resonance opens up the possibility of subsequent excitation to higher lying doubly excited resonances with a second tunable laser beam. In the future we hope to compare the angular momentum of the ejected electrons to that of nonresonant two-photon EPD.

We thank Bill Miller, Mark Gulley, and Dan Rislove for their technical assistance; Stan Schriber and David Schneider for access to the GTA; and J. Hontas, C. Allen, and J. DeMoss for technical expertise. H. C. B. and A. S. are supported by the Division of Chemical Sciences, Office of Basic Energy Sciences, Office of Energy Research, of the U.S. Department of Energy; X. M. Z., W. B. I., C. E. M. S., and D. J. F. under Contract No. W-7405-ENG.

[1] D. Proulx and R. Shakeshaft, Phys. Rev. A **46**, R2221 (1992).

[2] D. Proulx, M. Pont, and R. Shakeshaft, Phys. Rev. A **49**, 1208 (1994).

[3] For a very recent comparison of doubly excited states in the lithium and hydrogen ion see U. Berzinsh, G. Haeffler, D. Hanstorp, A. Klinkmüller, E. Lindroth, U. Ljungblad, and D. J. Pegg, Phys. Rev. Lett. **74**, 4795 (1995).

[4] M. Crance, J. Phys. B **21**, L557 (1988).

[5] M. Crance, J. Phys. B **23**, L285 (1990).

[6] H. K. Haugen, in *The Physics of Electronic and Atomic Collisions,* edited by T. Andersen, B. Fastrup, F. Folkmann, H. Knudsen, and N. Andersen, AIP Conf. Proc. No. 295 (AIP, New York, 1993), pp. 105–114.

[7] H. Stapelfeldt and H. K. Haugen, Phys. Rev. Lett. **69**, 2638 (1992).

[8] L. Sanche and P. D. Burrow, Phys. Rev. Lett. **29**, 1639 (1972).

[9] J. Callaway and A. R. P. Rau, J. Phys. B **11**, L289 (1978).

[10] H. C. Bryant, D. A. Clark, K. B. Butterfield, C. A. Frost, H. Sharifian, H. Tootoonchi, J. B. Donahue, P. A. Gram, M. E. Hamm, R. W. Hamm, J. C. Pratt, M. A. Yates, and W. W. Smith, Phys. Rev. A **27**, 2889 (1983).

[11] P. A. M. Gram, J. C. Pratt, M. A. Yates-Williams, H. C. Bryant, J. Donahue, H. Sharifian, and H. Tootoonchi, Phys. Rev. Lett. **40**, 107 (1978).

[12] The 35 keV injector was built for the ground test accelerator part of the NPB program supported by SDIO and BMDO.

[13] P. Kruit and F. H. Read, J. Phys. E **16**, 313 (1983).

[14] G. A. Kyrala and T. D. Nichols, Phys. Rev. A **44**, 1450 (1991).

[15] C. Blondel and C. Delsart, Nucl. Instrum. Methods Phys. Res., Sect. B **79**, 156 (1993).

[16] U. Fano, Phys. Rev. **124**, 1866 (1961).

[17] We thank R. Shakeshaft for kindly providing the calculated data shown in Fig. 3.

[18] K. R. Lykke, K. K. Murray, and W. C. Lineberger, Phys. Rev. A **43**, 6104 (1991).

[19] T. Scholz, P. Scott, and P. G. Burke, J. Phys. B **21**, L139 (1988).

[20] A. K. Bhatia and Y. K. Ho, Phys. Rev. A **41**, 504 (1990).

[21] Y. K. Ho, Phys. Rev. A **52**, 375 (1995).